

Variations in chain compactness and topological complexity uncover folding processes in the relaxation dynamics of unfolded in vacuo lysozyme

Gustavo A. Arteca, I. Velázquez, C. T. Reimann, and O. Tapia

Citation: *The Journal of Chemical Physics* **111**, 4774 (1999); doi: 10.1063/1.479240

View online: <http://dx.doi.org/10.1063/1.479240>

View Table of Contents: <http://scitation.aip.org/content/aip/journal/jcp/111/10?ver=pdfcov>

Published by the [AIP Publishing](#)

Articles you may be interested in

[Effects of knot type in the folding of topologically complex lattice proteins](#)

J. Chem. Phys. **141**, 025101 (2014); 10.1063/1.4886401

[Topology-based potentials and the study of the competition between protein folding and aggregation](#)

J. Chem. Phys. **130**, 115101 (2009); 10.1063/1.3089708

[Topological complexity, contact order, and protein folding rates](#)

J. Chem. Phys. **117**, 8587 (2002); 10.1063/1.1511509

[Finding the collapse-inducing nucleus in a folding protein](#)

J. Chem. Phys. **114**, 8678 (2001); 10.1063/1.1368134

[Conformation-dependent environments in folding proteins](#)

J. Chem. Phys. **114**, 2489 (2001); 10.1063/1.1338507



Variations in chain compactness and topological complexity uncover folding processes in the relaxation dynamics of unfolded *in vacuo* lysozyme

Gustavo A. Arteca

Département de Chimie et Biochimie, Laurentian University, Sudbury, Ontario, P3E 2C6 Canada

I. Velázquez

Department of Physical Chemistry, Uppsala University, Box 532, S-751 21 Uppsala, Sweden

C. T. Reimann

Division of Ion Physics, Department of Materials Science, Uppsala University, Box 534, S-751 21 Uppsala, Sweden

O. Tapia^{a)}

Department of Physical Chemistry, Uppsala University, Box 532, S-751 21 Uppsala, Sweden

(Received 7 May 1999; accepted 15 June 1999)

Chain collapse and the formation of a near-native tertiary structure are believed to be two key features controlling the progress of a protein folding transition. In this work, we study the interrelation between these two properties along computer-simulated relaxation trajectories of unfolded *in vacuo* lysozyme. Large-scale molecular shape transitions are monitored within a space defined by two discriminating descriptors of chain compactness and entanglement (or “topological”) complexity. For the system studied here, results indicate that successful refolding into native-like conformers requires a *balance* between polymer collapse and a topologically “correct” organization of chain loops. Although no single factor dominates the relaxation paths, compactization appears to be a necessary condition for near-native refolding. Whenever initial collapse is limited or absent, we find a “derailed” folding path with high configurational frustration. We also show that disulfide-reduced lysozyme unfolds differently, yet relaxes to the pattern of molecular shapes characteristic of the folded states of disulfide-intact lysozyme. © 1999 American Institute of Physics. [S0021-9606(99)50634-X]

I. INTRODUCTION

The folding transition taking a denatured protein to its native state does not proceed by random search in configurational space.¹ The current view suggests instead a nonrandom cooperative process involving a manifold of favored paths over a rugged landscape with a “downhill” bias.^{2–8} From the structural viewpoint, the transition is believed to involve both the formation of a compact globule and the development of structural organization at the local level (e.g., secondary structure, disulfide bridges).^{9,10} Yet, it is unclear whether secondary structure is formed progressively along the folding path or rather is initiated only after the formation of a structureless compact intermediate. Computer simulations with lattice and off-lattice models indicate that both scenarios are indeed possible depending on the strength of the interaction between residues.^{11–14} Protein folding appears to involve a subtle interplay between molecular size and compactness, on the one hand, and the chain topology, on the other hand.¹⁵ Capturing the relation between these two features is difficult, since the transition from a collapsed globule to a quasative state proceeds at virtually constant mean molecular size.¹⁴ A clear discrimination between the process of compactization by rapid collapse and chain reor-

ganization at constant size requires one to use shape descriptors that take into account both the geometry and the connectivity (i.e., the “topology”) of the protein chain. In this work, we address this issue by discussing some general aspects of the *in vacuo* folding–unfolding transition in a protein, employing a convenient molecular shape space¹⁶ that highlights the interrelation between compactness and chain topology.

The field of *in vacuo* protein dynamics has developed rapidly over the past few years. Various experimental techniques provide low-resolution glimpses of protein conformations *in vacuo* and in the gas phase.^{17–21} From a conceptual viewpoint, protein folding *in vacuo* is a key phenomenon within a general theory of protein folding. The notion of *in vacuo* folding would appear to challenge the view that regards solvent effects as necessary in driving conformational changes. However, native-like states in absence of solvent are still possible since collapse transitions can also take place *in vacuo*.²² In this work, we use computer simulations to uncover some features of the pattern of large-scale conformational changes that take place *in vacuo*. As a working system, we consider folding–unfolding transitions in lysozyme. Realistic simulations of *unfolding* of *in vacuo* lysozyme have been shown to be consistent with experiments that indicate the formation of elongated conformers.^{23–25} A recent study of the relaxation dynamics from unfolded conformers of disulfide-intact lysozyme sug-

^{a)}Author to whom correspondence should be addressed. Electronic mail: orlando.tapia@fki.uu.se

gests the occurrence of a well-defined folding process leading to long-lived compact structures, including native and quasistative states.²⁶ In the present work, we expand on this study by providing a first detailed analysis of how molecular compactness and chain entanglements evolve when relaxing partially unfolded conformers of *both* disulfide-intact and disulfide-reduced lysozyme. By using an ensemble of 19 nanosecond-long relaxation trajectories, we provide a qualitative overview of the configurational space accessible to lysozyme under nonstationary conditions. The work is organized as follows. In Sec. II, we review briefly the evaluation of molecular shape descriptors and the computational details for the molecular dynamics simulations. Results for the relaxation trajectories in disulfide-intact and disulfide-reduced lysozyme are discussed in Sec. III and IV, respectively. The closing section summarizes our observations in the broader context of what defines a folding process *in vacuo*.

II. MOLECULAR SHAPE SPACE AND COMPUTER-SIMULATED PROTEIN RELAXATION

The onset of chain collapse can be monitored with a shape descriptor of compactness. We use the *asphericity*,²⁷ given in terms of the principal moments of inertia $\{I_i\}$

$$\Omega = \frac{(I_2 - I_1)^2 + (I_3 - I_2)^2 + (I_3 - I_1)^2}{2(I_3 + I_2 + I_1)^2}.$$

The transition from prolate to spheroidal conformers appears as a change in asphericity from $\Omega \approx 1/4$ to $\Omega \approx 0$. The organization of the tertiary structure is more difficult to follow. If we restrict ourselves to large-scale molecular shape features, we can use *chain entanglements* to convey the topology of the backbone.^{16,28} A simple descriptor of entanglement complexity is the *mean overcrossing number* \bar{N} ,²⁸ defined as the number of bond–bond projected crossings (“overcrossings”), averaged over all spatial directions. By sampling a large number m of projections, and collecting the m_N projections yielding N overcrossings,²⁹ we have

$$\bar{N} = \lim_{m \rightarrow \infty} \sum_{N=0}^{\max N} N \frac{m_N}{m}, \quad \max N = (n-2)(n-3)/2$$

for an n -monomer chain.

The parameter \bar{N} can also be computed analytically, by using the geometry and connectivity of the backbone.³⁰ Self-entanglements characterize permanent^{31–33} and transient³⁴ topological constraints in biopolymers (e.g., DNA knots and polymer melts). Therefore, we use the term “topological complexity” when referring to a molecular shape characterization of a protein in terms of backbone entanglements. The (\bar{N}, Ω) -map defines a convenient molecular shape space to follow large-scale conformational rearrangements in proteins.

We have employed molecular dynamics (MD) to simulate the unfolding and relaxation of *in vacuo* lysozyme. The GROMOS87 (D4 parameter set) force field was used,³⁵ including polar hydrogens and a purely electrostatic description of hydrogen bonding.³⁶ Unfolded conformers for disulfide-intact and disulfide-reduced lysozyme were gener-

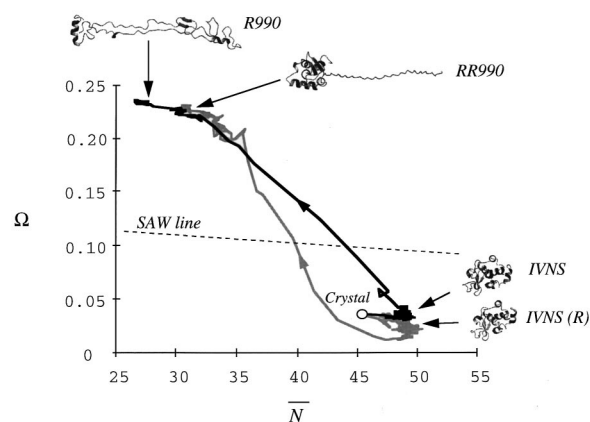


FIG. 1. Anisometry-and-entanglement molecular shape map for the unfolding trajectories of disulfide-intact (thick line) and disulfide-reduced (gray line) lysozyme. (The result for the crystal structure is denoted by an open circle. Snapshots are provided for the *in vacuo* native structures (bottom) and fully unfolded conformers (top). For reference, the dashed line represents the results for self-avoiding walks with 129 “monomers.” See the text.)

ated from the crystal structure (PDB code 1 hel, $n=129$ residues) under the effect of centrifugal forces.²³ Within the *in vacuo* boundary conditions, the whole system can rotate after equilibration. The resulting structures are the starting points for relaxation studies. It is important to contrast the two unfolding trajectories in shape space. As shown by the (\bar{N}, Ω) -map in Fig. 1, although both forms of lysozyme produce elongated conformers under denaturing conditions, their structure and unfolding mechanisms are significantly different. Prior to the onset of unfolding, the *in vacuo* native states of disulfide-intact and disulfide-reduced lysozyme [IVNS and IVNS(R), respectively] are similar. Both produce slightly larger chain entanglements with respect to the native state in the crystal, due to the constriction effect of the vacuum.²³ However, disulfide-reduced lysozyme has smaller Ω values, indicating that the lack of disulfide bridges lends the molecule some plasticity to reorganize itself more spherically. This initial difference propagates to the entire unfolding trajectory. Whereas disulfide-intact lysozyme evolves rapidly into an elongated “hairpin,” disulfide-reduced lysozyme maintains a spheroidal core and only unfolds a single strand. The snapshots in Fig. 1 illustrate the typical shapes of the conformers once full unfolding is reached. (Plots have been generated with the program MOLMOL.³⁷) To complete the comparison, Fig. 1 includes the results for the configurationally averaged shape parameters for self-avoiding walks (SAWs) in the continuum (dashed line).²⁸ Points along the “SAW line” correspond to 129-bead random walks with variable hard-sphere interaction. The line divides the (\bar{N}, Ω) space into zones where repulsion and attraction dominate (above and below the line, respectively). This line identifies the region of interest to study relaxation transitions. Intuitively, we would expect that the relaxation of unfolded conformers below the SAW line should tend to produce refolding. In contrast, such a behavior would by no means be ensured for the relaxation of unfolded conformers found above the dashed line (i.e., those found in the repul-

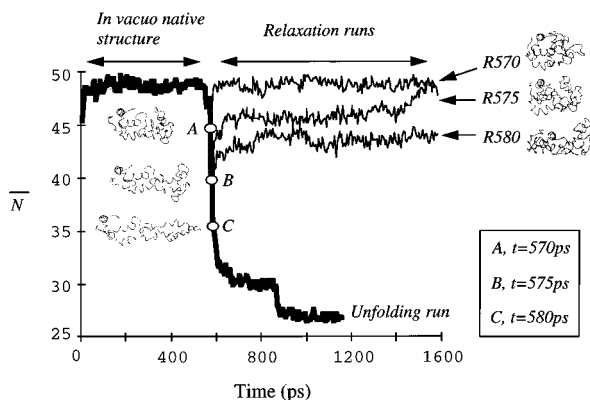


FIG. 2. Variation of mean overcrossing number along the unfolding (thick line) and selected relaxation (thin lines) trajectories of disulfide-intact lysozyme. The circles denoted by A, B, and C represent initial transients along the unfolding run used for relaxation.

sive regime, therefore with significant conformational distortions).

Relaxation trajectories have been generated following the procedure in Ref. 26. The essential details are as follows. For each conformer, unfolding conditions are switched off, velocities are rerandomized, and the whole system is weakly coupled to a Berendsen thermostat at $T=293$ K.³⁸ Temperature is kept constant during the relaxation simulations. No periodic boundary conditions are imposed, and a 1.3 nm cut-off is used for Coulomb interactions. Relaxation trajectories are followed for at least 1.0 ns. As initial “seeding” structures, we have considered several conformers of disulfide-intact and disulfide-reduced lysozyme, placed within the region for fast unfolding (i.e., near the dashed line in Fig. 1). Unfolded conformers for disulfide-intact and disulfide-reduced lysozyme are denoted by “Rxxx” and “RRxxx,” respectively, where “xxx” indicates the time in picoseconds from the beginning of the unfolding simulation. The corresponding MD relaxation trajectories are labeled likewise.

III. RELAXATION AND REFOLDING OF DISULFIDE-INTACT LYSOZYME

Significant “seeds” for relaxation studies of disulfide-intact lysozyme are found within the period $t=570$ ps and $t=580$ ps along the unfolding run. (Some representative seeds are indicated by the A, B, and C dots in Fig. 2, together with their corresponding ribbon structures.) During these 10 ps, molecular size increases by 40%. Relaxation trajectories starting from these transients lead to a variety of intermediates, some of which persist for almost 1 ns. Unfolded transients found for $t<570$ ps exhibit small distortions and quickly relax back to the native state.

We have found structures above and below the SAW line. The former are referred to as *noncompact structures*, whereas the latter form a class of *compact structures*.

Figure 2 illustrates how chain entanglements evolve during relaxation. (The thick line represents the unfolding trajectory, whereas the relaxation runs appear in thin lines.) At least two families of conformations can be recognized. Whereas the R570 trajectory leads back to \bar{N} values typical

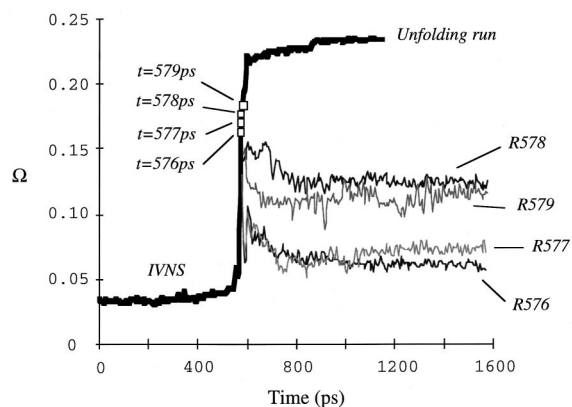


FIG. 3. Variation of asphericity along the unfolding (thick line) and selected relaxation (thin lines) trajectories of disulfide-intact lysozyme. Squares denote initial transients.

of the *in vacuo* native state, the R580 trajectory stabilizes in a state with fewer entanglements. The R575 trajectory shows an intermediate behavior, in the sense that \bar{N} changes smoothly from a region characterized by low entanglement to a region associated with the *in vacuo* native state (i.e., higher entanglement). These results are representative of a pattern of clustering observed as unfolded transients are allowed to relax. This situation is further illustrated in Fig. 3 using now the variation in chain compactness for relaxation trajectories starting from four transients differing in 1 ps along the unfolding run (i.e., from R576 to R579). The runs starting from more distorted initial structures (R578 and R579) behave similarly and cluster around the results observed for the R580 trajectory. These trajectories do not lead back to native or quasinaive conformers, but instead give rise to persistent *noncompact* intermediates (located over the SAW line in Fig. 1). In contrast, the final results for the R576 and R577 runs cluster around those for the R575 trajectory and correspond to *folded*, albeit *denatured*, conformers, located within the region of *compact* intermediates (i.e., below the SAW line in Fig. 1). Some of these *folded denatured* conformers persist for almost 1 ns, whereas other evolve towards *quasinaive* conformers. (Quasinaive configurations have compactness and topological complexity similar to that of the native state, despite differences in the details of the tertiary structure.) The difference between these two families of relaxed conformers shown in Fig. 3 is sharp; our results indicate no intermediate behavior.

This clustering pattern is further highlighted when all relaxation trajectories are observed in shape space. Figure 4 collects the 11 relaxation runs from R570 to R580, starting from unfolding transients separated by 1 ps. Squares indicate the initial structures for relaxation, whereas circles (error bars) indicate the location (fluctuations) of any significant persistent intermediate found within 1 ns. Lines represent the approximate path followed from the initial structure to the final intermediate. For completeness, the intermediates observed along each of the relaxation paths are summarized in Table I. Regarding the general relaxation behavior of disulfide-intact lysozyme, we can make the following observations:

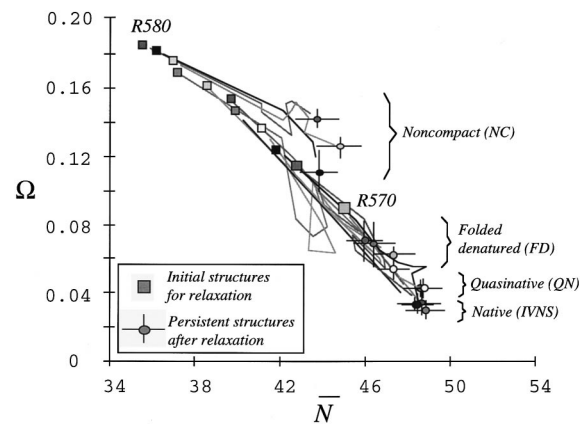


FIG. 4. Molecular shape map for all relaxation trajectories of disulfide-intact lysozyme. (See Table I for the correspondence between initial transients and final structures.)

- (a) For all initial transients with $t \leq 577$ ps, the relaxation runs trace qualitatively (in reverse) the unfolding path. Along the relaxation paths, we observe a balance between the increase in compactness and the development of chain entanglements. All these paths lead back to compact persistent intermediates, although not necessarily quasinate.
- (b) The relaxation paths starting from $t > 577$ ps transients do not traverse the swath of configurations representative of the unfolding path. As their main characteristic, these paths exhibit *slow* compactization of the backbone (note the slopes in Fig. 4), and do *not* lead to compact persistent structures. By not engaging in rapid collapse, these relaxations appear to produce intermediates with higher configurational frustration than those in (a) (i.e., persistent intermediates located over the SAW line).
- (c) The $R576$ and $R577$ relaxation runs exhibit instances of rapid collapse, as identified by a sudden decrease in asphericity. However, this decrease is arrested before the transients reach quasinate compactness. Instead, the conformers rearrange their tertiary structure,

TABLE I. Persistent structures obtained after 1 ns relaxation runs starting from different *in vacuo* unfolded conformers of lysozyme, with and without disulfide bridges. (Symbols $Rxxx$ and $RRxxx$ identify the relaxation runs for disulfide-intact and disulfide-reduced lysozyme, respectively, starting from the transient found at $t = xxx$ ps along the unfolding trajectory. The symbols N, QN, FD, and NC stand for native, quasinate, folded denatured and noncompact conformers. An arrow connecting two types of conformers indicates that both are found to persist for some amount of time along the corresponding relaxation path.)

Starting structure (disulfide-intact)	Final structure (disulfide-intact)	Starting structure (disulfide-reduced)	Final structure (disulfide-reduced)
$R570$	N[IVNS]	$RR697$	N[IVNS(R)]
$R571$	N[IVNS]	$RR700$	N[IVNS(R)]
$R572$	N[IVNS]	$RR705$	QN
$R573$	FD→QN	$RR710$	QN→N[IVNS(R)]
$R574$	N[IVNS]	$RR715, R720$	QN
$R575$	FD→QN	$RR725$	NC→FD
$R576, R577$	FD	$RR730$	NC
$R578, R579, R580$	NC		

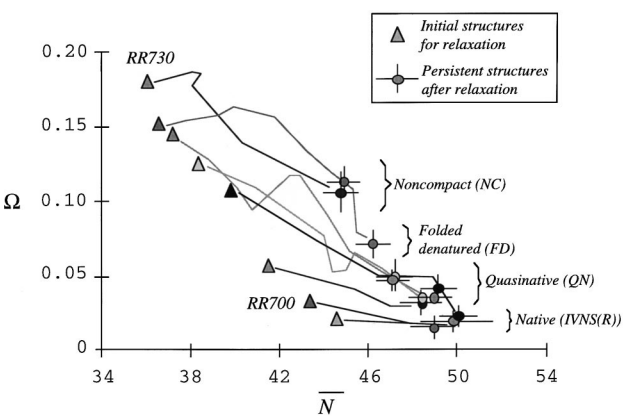


FIG. 5. Molecular shape map for all relaxation trajectories of disulfide-reduced lysozyme. (See Table I for the correspondence between initial transients and final structures.)

- thereby increasing their asphericity with a minimum change in topological complexity. By doing so, the conformers appear to “inflate” back towards the shapes found along the unfolding path. (A similar phenomenon is observed when relaxing strongly elongated, fully unfolded transients.²⁶) By following this behavior, the $R577$ trajectory appears to have avoided being “derailed” into the noncompact folded intermediates in (c). This observation is again consistent with the notion that instances of rapid collapse may be needed to generate compact intermediates.^{9–14}
- (d) Results in Table I and Fig. 4 are consistent with a rugged energy landscape for folding.^{39,40} There is no simple correspondence between how distorted an initial transient is and how compact (and entangled) the final intermediate is. For instance, whereas $R573$ leads to folded denatured and quasinate conformers, the more distorted initial transient $R574$ leads back to the native structure (see Table I). Similar crossovers have been found in simulations of unfolding.⁴¹

Despite the difference in detail among the trajectories, our results point towards a common pattern of protein relaxation, i.e., a folding process. We find no evidence of random search in the shape space of (*a priori*) uncorrelated descriptors \bar{N} and Ω . Certain molecular shapes and shape transitions appear to be favored over others. In particular, relaxation processes involving the formation of high entanglement with a minimal amount of compactization do not seem to be consistent with rapid refolding.

IV. RELAXATION OF DISULFIDE-REDUCED LYSOZYME

Disulfide-reduced lysozyme follows another unfolding path, thus probing a distinct ensemble of initial configurations for relaxation. In this case, we find elongated conformers that retain a compact domain with residual secondary structure. By using a similar approach to that in Sec. III, we have tested whether a pattern emerges during their relaxation.

Figure 5 presents the results of eight relaxation trajec-

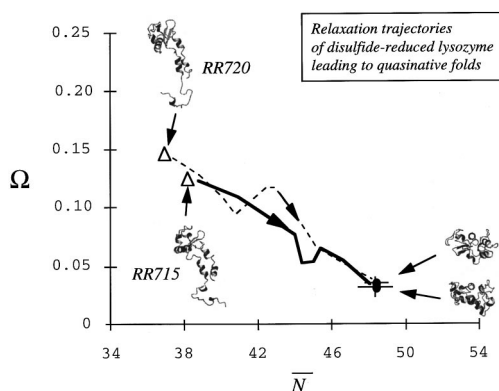


FIG. 6. Selected relaxation trajectories of disulfide-reduced lysozyme exhibiting oscillations in compactness. (Snapshots correspond to initial transients and final structures.)

ries, started from initial configurations among transients with $t = 697$ ps and $t = 730$ ps along the unfolding run. (This range is qualitatively similar to the one used in Sec. III.) As in Fig. 4, the (\bar{N}, Ω) -map includes the approximate paths linking the initial conformers to the final persistent intermediates. Table I completes the information by listing the nature of the final conformers for each relaxation run. We can make the following observations regarding the relaxation pattern for disulfide-reduced lysozyme:

- As found in Sec. III, persistent intermediates cluster again into groups spanning a range of molecular shapes, including both native and non-native structures.
- Only the trajectories starting from minimally unfolded conformers (RR697 and RR700) trace in reverse the unfolding path. All other relaxation runs follow a different behavior, exhibiting a faster increase in chain entanglement rather than rapid compactization.
- We find evidence of transient, sudden collapse for relaxation trajectories started from significantly unfolded conformers. Figure 6 highlights this behavior for the RR715 and RR720 trajectories. Although the extent of the collapse is smaller than the one observed in Fig. 4, these trajectories also lead to quasinative conformers.
- Relaxation runs started from strongly unfolded conformers can evolve with *no initial compactization* (e.g., the RR725 and RR730 trajectories). These trajectories produce *noncompact* or *folded denatured* structures, rather than quasinative conformers. These results are consistent with those in Sec. III, where relaxation with minimal initial collapse is found to “derail” (at least temporarily) the folding path towards states with configurational frustration.

The most striking observation can be made from Fig. 7, which superimposes the relaxation trajectories for both forms of lysozyme. As the figure shows, the relaxation of disulfide-reduced lysozyme does not trace back its corresponding unfolding run but rather “crosses” rapidly into the swath of molecular shapes characteristic of the relaxation of disulfide-intact lysozyme. Despite the difference in initial transients for relaxation, there is a close match between the

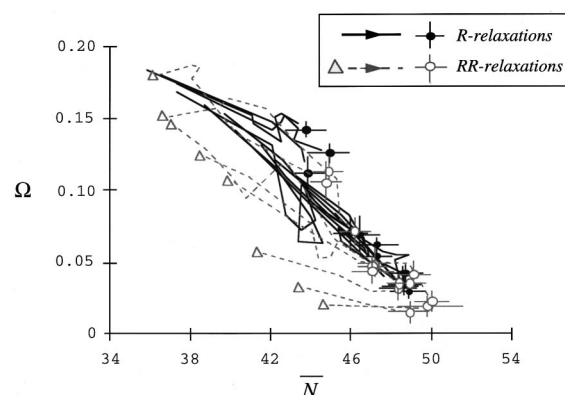


FIG. 7. Molecular shape map for all relaxations of lysozyme. (R- and RR-relaxations correspond to disulfide-intact and disulfide-reduced lysozyme, respectively. Note that the trajectories for disulfide-reduced lysozyme do not trace back their unfolding run, but rather cross into the regime of molecular shapes characteristic of folded disulfide-intact lysozyme.)

final (persistent) structures found in both cases. (This similarity must be understood strictly in terms of *global* molecular shape features. Actual root-mean-square deviations between individual structures can be large.) Note that the similarity of molecular shape features extends to both compact and noncompact intermediates. This result suggests that the formation of disulfide bridges may not be a necessary condition to drive the folding of lysozyme towards quasinative conformers. Rather, the capability of forming protein globules with near-native compactness and topology appears to be intrinsic to this primary sequence. It is possible that having the correct compactness and topological complexity could facilitate the formation of disulfide bridges, given the right chemical conditions.

V. FURTHER COMMENTS AND CONCLUSIONS

Our results indicate a systematic interrelation between the evolution of chain compactness and chain entanglement during protein relaxation. We believe that the pattern observed is the mark of an organized folding process *in vacuo*.²⁶ Our work provides an insight into this process: we find that relaxation paths with *slow compactization* appear to increase the configurational frustration rather than lead to compact intermediates. This observation is consistent with the notion that protein collapse is the favored *first folding step* whenever the effective interaction between residues is strongly attractive.^{12,13} It is conceivable that our simulations are found in this regime, since *in vacuo* interactions have minimum screening.

Our results reinforce the notion that one must use a significant ensemble of trajectories in order to identify global trends in nonstationary processes.⁴¹ In the present case, the trajectories have been generated from a set of variable initial configurations with an unfolding bias. Otherwise, the initial distribution of velocities for the MD simulations has been generated with the same procedure and the same random seeds.

The availability of a concise and informative shape space is central to our analysis. An (\bar{N}, Ω) -map is well adapted to following the formation of large-scale features

during configurational rearrangements. The approach allows one to recognize the onset of chain compactness, as well as the evolution of the backbone topological complexity. As noted elsewhere,¹⁵ these properties may be more important than molecular size when attempting to develop a model for protein folding rates. In this context, an (\bar{N}, Ω) -map serves as a convenient shape space out of which interconversion (reaction) coordinates can be defined. It remains to be seen, however, whether this space satisfies more stringent criteria for selecting a “good” coordinate to be used in protein folding.⁴²

ACKNOWLEDGMENTS

G.A.A. thanks the NSERC (Natural Sciences and Engineering Research Council of Canada) for support, C.T.R. thanks the TFR (Swedish Technical Research Council), and O.T. is grateful to the NFR (Swedish Natural Sciences Research Council) for financial support.

- ¹C. Levinthal, in: *Mössbauer Spectroscopy of Biological Systems* edited by P. Debrunner, J.-C. Tsibris, and E. Munck (University of Illinois Press, Urbana, 1969).
- ²M. Karplus and E. I. Shakhnovich, in: *Protein Folding*, edited by T. Creighton (Freeman, New York, 1992).
- ³R. Baldwin, *Nature (London)* **369**, 183 (1994).
- ⁴J. Bryngelson, J. N. Onuchic, N. D. Socci, and P. G. Wolynes, *Proteins: Struct., Funct., Genet.* **21**, 167 (1995).
- ⁵A. R. Fersht, *Curr. Opin. Struct. Biol.* **7**, 3 (1997).
- ⁶K. A. Dill and H. S. Chan, *Nat. Struct. Biol.* **4**, 10 (1997).
- ⁷S. Takada and P. G. Wolynes, *Phys. Rev. E* **55**, 4562 (1997).
- ⁸C. M. Dobson and M. Karplus, *Curr. Opin. Struct. Biol.* **9**, 92 (1999).
- ⁹K. Dill, *Biochemistry* **24**, 1501 (1985).
- ¹⁰H. Orland, C. Itzykson, and C. De Dominicis, *J. Phys. (France) Lett.* **46**, L353 (1985).
- ¹¹A. M. Gutin, V. I. Abkevich, and E. I. Shakhnovich, *Biochemistry* **34**, 3066 (1995).
- ¹²V. I. Abkevich, A. M. Gutin, and E. I. Shakhnovich, *J. Mol. Biol.* **252**, 460 (1995).
- ¹³S. He and H. A. Scheraga, *J. Chem. Phys.* **108**, 287 (1998).
- ¹⁴A. Gutin, A. Sali, V. Abkevich, M. Karplus, and E. I. Shakhnovich, *J. Chem. Phys.* **108**, 6466 (1998).
- ¹⁵K. W. Plaxco, K. T. Simons, and D. Baker, *J. Mol. Biol.* **277**, 985 (1998).
- ¹⁶G. A. Arteca, *Biopolymers* **35**, 393 (1995); *Macromolecules* **29**, 7594 (1996).
- ¹⁷D. S. Gross, P. D. Schnier, S. E. Rodríguez-Cruz, C. K. Fagerquist, and E. K. Williams, *Proc. Natl. Acad. Sci. USA* **93**, 3143 (1996).
- ¹⁸K. Shelimov and M. F. Jarrold, *J. Am. Chem. Soc.* **118**, 10313 (1996); *ibid.* **119**, 2987 (1997).
- ¹⁹J. S. Valentine, J. G. Anderson, A. D. Ellington, and D. E. Clemmer, *J. Phys. Chem. B* **101**, 3891 (1997).
- ²⁰F. W. McLafferty, Z. Guan, U. Haupts, T. D. Wood, and N. L. Kelleher, *J. Am. Chem. Soc.* **120**, 4732 (1998).
- ²¹C. T. Reimann, P. A. Sullivan, J. Axelsson, A. P. Quist, S. Altman, P. Roepstorff, I. Velázquez, and O. Tapia, *J. Am. Chem. Soc.* **120**, 7608 (1998).
- ²²P. G. Wolynes, *Proc. Natl. Acad. Sci. USA* **92**, 2426 (1995).
- ²³C. T. Reimann, I. Velázquez, and O. Tapia, *J. Phys. Chem. B* **102**, 2277 (1998).
- ²⁴C. T. Reimann, I. Velázquez, and O. Tapia, *J. Phys. Chem. B* **102**, 9344 (1998).
- ²⁵M. Marchi and P. Ballone, *J. Chem. Phys.* **110**, 3697 (1999).
- ²⁶G. A. Arteca, I. Velázquez, C. T. Reimann, and O. Tapia, *Phys. Rev. E* **59**, 5981 (1999).
- ²⁷A. Baumgärtner, *J. Chem. Phys.* **98**, 7496 (1993).
- ²⁸G. A. Arteca, *Biopolymers* **33**, 1829 (1993); *Phys. Rev. E* **49**, 2417 (1994).
- ²⁹G. A. Arteca and P. G. Mezey, *Biopolymers* **32**, 1609 (1992).
- ³⁰G. A. Arteca and D. I. Caughill, *Can. J. Chem.* **76**, 1402 (1998); G. A. Arteca, *J. Chem. Inf. Comp. Sci.* **39**, 559 (1999).
- ³¹V. Katritch, J. Bednar, D. Michoud, R. G. Scharein, J. Dubochet, and A. Stasiak, *Nature (London)* **384**, 142 (1996).
- ³²A. Stasiak, V. Katritch, J. Bednar, D. Michoud, and J. Dubochet, *Nature (London)* **384**, 122 (1996).
- ³³A. V. Vologodskii, N. J. Crisona, B. Laurie, P. Pieranski, V. Katritch, J. Dubochet, and A. Stasiak, *J. Mol. Biol.* **278**, 1 (1998).
- ³⁴A. L. Kholodenko and T. A. Vilgis, *Phys. Rep.* **298**, 251 (1998).
- ³⁵W. F. van Gunsteren and H. J. C. Berendsen, *Groningen Molecular Simulation-GROMOS Library Manual* (Biomos, Groningen, 1987).
- ³⁶J. Åqvist, W. F. van Gunsteren, M. Leijonmarck, and O. Tapia, *J. Mol. Biol.* **83**, 461 (1985).
- ³⁷R. Koradi, M. Billeter, and K. Wüthrich, *J. Mol. Graphics* **14**, 51 (1996).
- ³⁸H. J. C. Berendsen, J. P. M. Postma, W. F. van Gunsteren, A. DiNola, and J. R. Haak, *J. Chem. Phys.* **81**, 3684 (1984).
- ³⁹J. D. Bryngelson and P. G. Wolynes, *Proc. Natl. Acad. Sci. USA* **84**, 7524 (1987); *J. Phys. Chem.* **93**, 6902 (1989).
- ⁴⁰P. G. Wolynes, *Proc. Natl. Acad. Sci. USA* **94**, 6170 (1997).
- ⁴¹T. Lazaridis and M. Karplus, *Science* **278**, 1928 (1997).
- ⁴²R. Du, V. S. Pande, A. Yu. Grosberg, T. Tanaka, and E. I. Shakhnovich, *J. Chem. Phys.* **108**, 334 (1998).